ICAS 2021 SHANG HAI
International Council of the Aeronautical Sciences
32nd Congress of the International Council of the Aeronautical Sciences
September 6-10, 2021
Pudong Shangri-La, Shanghai, China

# Optimisation of Vortex Generators for Stall Speed Reduction

Jannek Meyer[1,2], Patrick Okfen[1,2], Cees Bil[2]

[1]Faculty of Aerospace Engineering, FH Aachen, Aachen, Germany
[2]School of Engineering, RMIT University, Melbourne, Australia

## Abstract

To make the Cessna 208 Caravan more suitable for the challenging missions of MAF International in Papua New Guinea, where short runways and tall surroundings necessitate high lift at low speeds, the application of vortex generators was investigated. An extensive literature review revealed eight geometric or direct design parameters which could be attributed to different physical effects. These could subsequently be condensed into three indirect design parameters governing vortex generator design, namely range of efficacy, kinematic energy input and drag. It was determined that strong interdependencies between the direct design parameters necessitate a numerical study to cover the entire design space. Optimisation via surrogate modelling was identified as a suitable approach. After 3D-Laser scanning the geometry, preliminary CFD studies hinted at limited potential for lift increase, as little flow separation was observable. Design optimisation of a Kriging surrogate model based on 60 sampling points confirmed these assumptions yielding a maximum lift increase of 1.22% at an angle of attack of 14°.

**Keywords:** vortex generators, optimization, stall speed, retrofit, CFD

## 1. Introduction

Mission Aviation Fellowship (MAF) International operates 128 aircraft in 27 countries around the world. To the many remote communities of Papua New Guinea, they provide access to medical services, schools, development agencies and church leadership [1]. The missions are particularly demanding because of high altitude, mountainous terrain, short and rough runways and adverse weather conditions (Figure 1). Aircraft operated in and out of these areas need to be able to take-off and land at low speeds and have good climb performance. The mission profile of MAF International is versatile but typically consists of short hops between communities. This means very little time is spent in cruise and take-off, climb and landing are dominant. The Cessna 208 Caravan is one of the aircraft used by MAF International for these missions. The aim of this project is to investigate the potential for lift increase at low speeds for the Cessna 208 with retrofit of passive vortex generators. As MAF performs landing and take-off with flaps fully extended, this is the configuration analyzed in this study.

Figure 1 – MAF Operating Environment.

Vortex generators (VGs) have been applied as a tool for passive flow control since the 1940s [2]. They represent a low-cost and versatile method for separation control in subsonic flow in adverse pressure gradients, as well as for delaying shock induced separation in transonic flows [3]. Delay of flow separation, or stall, is achieved by enhancing the momentum exchange between the low velocity region close to the wing surface and regions with higher flow velocity. This re-energises the low-energy boundary layer flow and reduces its separation affinity [2][4]. A secondary effect is excitement of local instability waves, which leads to an earlier transition to turbulent flow. As turbulent flow carries more kinetic energy compared to laminar flow, separation is also delayed [3].

Figure 2 shows a general schematic of vortex generators on a plate. During the design process of passive flow control devices like VGs, advantages such as low weight and relative simplicity are to be weighed against potential performance degradation at off-design conditions [5]. Rectangular vanes with a height similar to the local boundary layer thickness were the first designs applied for flow separation control [6]. An exploratory study points toward potential benefits of submerging vortex generators within the boundary layer, so-called micro VG [7]. While they show similar efficacy in delaying flow separation compared to conventional vortex generators, the incurred drag penalty is substantially lower [7].

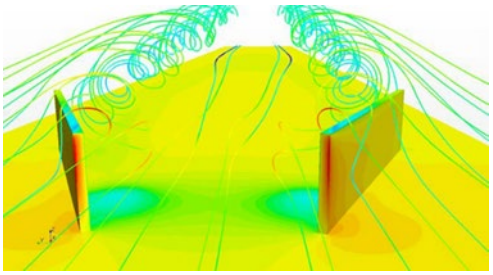

Figure 2 - Generic vortex generators flow visualisation [8].

The principal effect of vortex generators is the delay of flow separation. Application objectives range from drag reduction for low-Reynolds Number airfoils, separation control for high-lift devices, and increase of maximum lift coefficient. Application of low-profile VGs for low-Reynolds Number airfoils (chord Re < $10^6$) was also studied [9]. At angles of attack well below stall, a separation bubble forms just after the suction peak. A rapid transition into turbulent flow and consequent reattachment limit its impact on overall lift, but excess drag due to a thicker, turbulent boundary layer is the result. This wind tunnel study was performed at a maximum speed of 34 m/s and 2 x $10^5$ < Re < 6 x $10^5$ at $a$ = 4° [9]. At lift coefficient $c_l$ = 0.572, the application of low-profile VGs lead to a maximum reduction of drag by 38%. For high lift configurations, the risk of flow separation at low angles of attack prevails. High-lift systems which comprise airfoils with extended slats and flaps, show an affinity for flow separation on the flaps at low angles of attack which poses a serious risk to lift generation [2]. To mitigate this risk, it is suggested to mount low-profile VGs just downstream of the flap leading edge to maintain attached flow at low angles of attack [6]. This way high-lift devices become more suitable for a wider range of operational states as enhanced lift may be retained even at low angles of attack.

Interest in vortex generator research is rooted in their many practical applications. Examples range from small general aviation aircraft, military aircraft and large commercial aircraft like the Boeing 737 or 777 [10].The Embraer Legacy 500 has co-rotating trapezoidal VGs installed on the spanwise mid-section of its wing while the Gulfstream G550 utilises trapezoidal co rotating VGs near the wing tip. Retrofit VG kits are offered for a multitude of aircraft [11]. For the Cessna 207, an aircraft similar in size to the Cessna 208, a stall speed reduction of 8% is quoted [12].

## 2. Design of vortex generators

The design of VGs involves many different design parameters. A thorough literature review, e.g. [3] and [6], pointed at eight geometric parameters that should be taken into account when designing vortex generators:

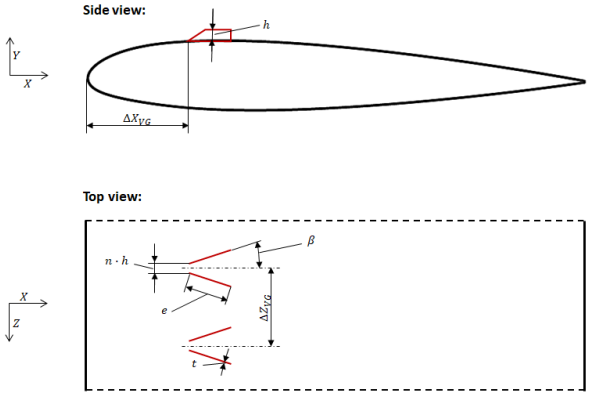


Figure 3 – Definition VG Design Parameters.

- VG type (e.g. forwards wedges or triangular counter-rotating vanes)
- VG height, usually given relative to the local boundary layer thickness: $h/\delta$
- VG length, usually given relative to the VG height: $e/h$
- VG orientation $\beta$
- VG thickness t
- Spanwise spacing between VG pairs, usually given relative to the VG height: $\Delta z_{VG}/h$
- Spanwise spacing between the different parts of a VG pair, usually given as multiple of the device height: $n$

- Chordwise VG position, in this paper defined as projected distance in $X$ direction between wing leading edge and VG leading edge relative to the VG height: $\Delta X_{VG}/h$

An illustration of how these design parameters have been used in this study is given in Figure 3. Consider that this definition varies slightly from literature to be more convenient for trapezoidal VGs rather than triangular VGs. In this study the VG height is measured at 50 % VG length and the chordwise position refers to the leading edge of the VGs rather than the trailing edge. Furthermore, the VG length is measured from the point where the VG leading edge touches the wing surface to the point where the VG trailing edge connects to the wing surface.
Partly inspired by the findings in [5] it can be concluded that these eight design parameters, trigger the following three physical effects: the range of efficacy of the created vortices, the kinetic energy input into the momentum transfer and the device drag. The Range of efficacy defines the streamwise distance behind the VG device at which the created vortices have sufficient strength to facilitate the momentum exchange between the different flow layers (Figure 4). There are two factors that influence the range of efficacy which are the initial vortex strength and the vortex decay. Since the separation line, i.e. the connection in spanwise direction of all flow separation points, is not fixed in many real-world applications, a large range of efficacy ensures a robust design, suitable for a wide range of operational states. Also, if the separation line is not known a large range of efficacy is beneficial. The kinetic energy input describes the kinetic energy in the flow just upstream of the device which is available for the conversion into vorticity. It depends on the constitution of the boundary layer at the respective chordwise VG location (Figure 4). Drag is generally attributable to a lot of different factors. The main contributors are friction and the conversion of aircraft forward momentum into unrecoverable wake drag [18].

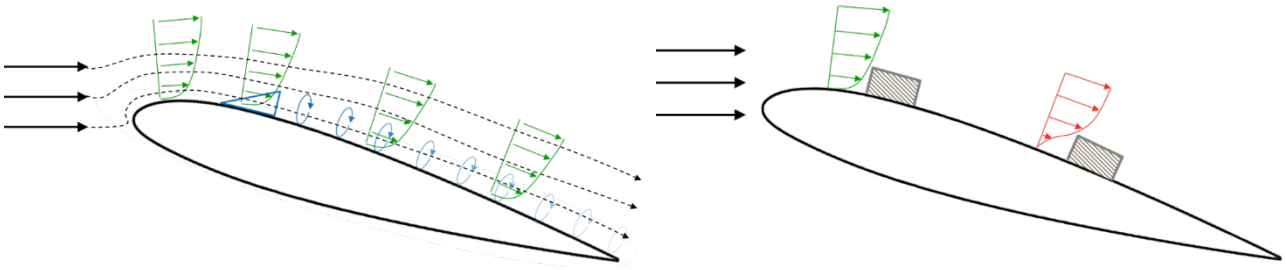

Figure 4 - Illustration range of efficacy (left) and kinetic energy input (right).

The three principal effects shall be referred to as indirect design parameters in the following since they are based on the physical effects VGs induce in the flow filed. In contrast the geometric parameters will be referred to as direct design parameters. Figure 5 shows the relationship of the two types of design parameters and thus explains how the direct design parameters influence the vortex formation and propagation.
The eight direct design parameters are highly interdependent which makes it extremely hard to size the different parameters separately. Without claiming to be exhaustive, Figure 6

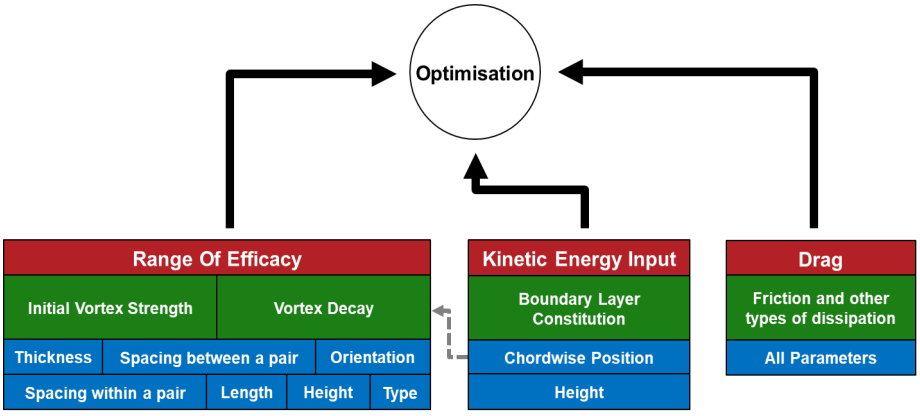


Figure 5 - Direct design parameters (blue) allocated to the indirect design parameters (red) and the underlying physical effects (green).

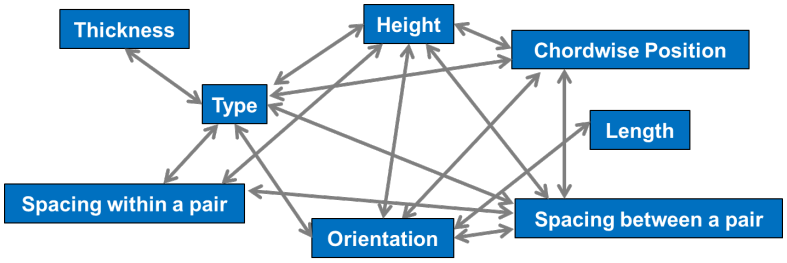


Figure 6 - Interdependencies of VG design parameters.

shows a variety of interdependencies that must be considered when designing vortex generators.
Due to this high interdependency between the design parameters, the wide range of possible VG applications and the required trade-off between drag and momentum exchange, design guidelines cannot easily be stated. Instead an optimisation is required that utilizes a deep understanding of vortex generators to guide the optimisation.
As shown by [3], experimental optimisation via parametric design can yield useful results when focusing on one parameter. However, time constraints and the number of governing design parameters limit the optimisation potential. These constraints may be overcome by numerical optimisation schemes, which can incorporate multiple parameters simultaneously and cover a vast design space more efficiently. However, a limited capability to model flow separation must be considered.

## 3. Methodology

To evaluate the potential for stall speed reduction of the Cessna 208 by a VG retrofit, the methodology outlined in Figure 7 was applied. As neither geometric nor aerodynamic data was available as a basis, an approach starting from scratch was necessary. Note that not all steps are discussed in detail in this paper.
The first step was a thorough literature review. Subsequently, the number of relevant direct VG design parameters (Figure 3) and their respective boundaries, the so-called preliminary design space, were determined.
In the third step, 3D laser scanning was employed to reverse-engineer the wing geometry with flap. Particularly accurate modelling the wing – flap cavity was essential.
The obtained geometrical information was used to design parametrised CAD models that allow for both 2D and 3D CFD analysis of relevant cross sections applying automatic meshing tools. Once the CFD framework was set up, a CFD validation study was conducted to ensure 2D airfoil flow physics are represented with confidence. In the following the aerodynamic performance of two representative cross section (flaps fully extended) was evaluated to establish a baseline for the subsequent optimisation process. This step was essential and had to be conducted thoroughly as no baseline aerodynamic data is available for the simulated configurations.
In a next step the mesh for a 3D section with a single pair of installed VGs was set up and optimised. At this stage, the computational resources required per design parameter combination eventually became clear thus the scope of optimisation and the final design space could

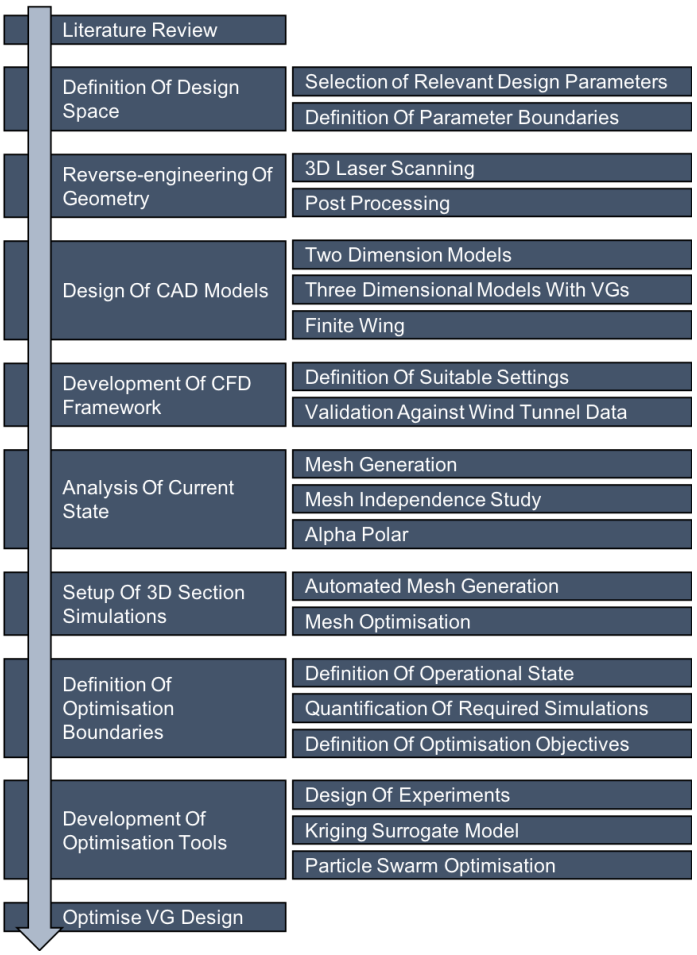


Figure 7 – Flow Diagram for VG Design Optimisation.

be defined. Due to computational limitations VG optimisation had to be limited to a 2.5D section and a single operational state.
After CFD tools as well as numerical optimisation tools (Latin Hypercube Sampling, Kriging Surrogate Modelling and Particle Swarm Optimisation) were setup the VG optimisation could be performed. A sampling plan was generated as part of the design of experiments, CFD simulations were conducted, a Kriging model was constructed based on the simulation results and the particle swarm optimisation algorithm was run in order to find an optimum configuration.

## 4. CFD Framework and Meshing

### General Setup

The CFD framework must be capable of capturing a variety of different flow conditions. Important is the accurate resolution of flow separation, slot flow, vortex formation and vortex propagation at low flight speeds. However, aerodynamic optimisation of a wing asks for a multitude of CFD simulations to be performed, making an accurate but efficient CFD framework essential.
A bullet shaped flow domain was chosen with a maximum size in chordwise and vertical direction of 40 times the chord length. ANSYS Meshing was used to generate all triangular 2D meshes and ANSYS FLUENT Meshing was utilised for creating the 2.5D polyhedral meshes. In all meshes the wake region was refined depending on the angle of attack, the leading edge was refined to account for the high velocity gradients and the trailing edge was refined to prevent the occurrence of numerical instabilities due to poor quality cells. In general, the upper airfoil surface was more finely meshed compared to the lower side as the intended installation of the VGs on the upper side demanded higher accuracy. To achieve a precise resolution of the boundary layer the first prism height was chosen to correspond to a $y^+ < 2$ in all flow regions. The total prism height was defined to cover the entire boundary layer based on an approximation of fully turbulent flow along a flat plate. For a fine mesh, these settings cause an undesirably high aspect ratio of the prism cells which was counteracted by placing as many as 42 prism layers around the airfoil. The set-up and solution settings were chosen as presented in Table 1.

Table 1 - CFD settings.

| | |
|---|---|
| Equation type | RANS |
| Compressibility | Incompressible => energy equation off |
| Time dependence | Steady or transient |
| Solver category | Pressure-based |
| Solver | SIMPLE |
| Under-relaxation factors | default |
| Spatial-discretisation | Second-order-Upwind |
| Timewise discretisation (only for transient) | Implicit Second-order |
| Turbulence model | SST k-$\omega$ with curvature correction |
| Transition model | Intermittency Transition model |
| Velocity | 31.389 m/s |
| Pressure | 1.01325 bar |
| Temperature | 15 °C |
| Density | 1.225 kg/m³ |
| Turbulence intensity | 5 % |
| Turbulence viscosity ratio | 10 |

### Validation of the CFD framework against wind tunnel data

In order to assure physical validity of the results, the CFD framework was validated against NACA wind tunnel data [21]. As the Cessna 208 has aerodynamic twist between the NACA 23012 and the NACA 23017.424, the NACA 23015 gives a good representation of the prevailing flow characteristics.
In a first step a mesh independence study was performed for an angle of attack of 12.1°. As simulations in the stall region usually require a relatively high cell count, grid independence at a large angle of attack

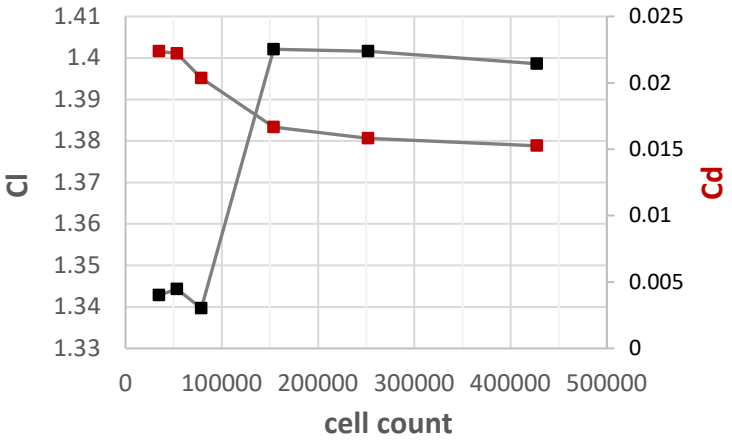


Figure 8 - Grid independence study.

is assumed to be sufficient for analysing all relevant angles of attack (Figure 8).
The mesh comprising 150000 cells is considered reasonably accurate as the deviation in Cl is only 0.2 % when compared to the finest mesh. The drag coefficient deviates by 9 % which is acceptable since the solution for lift is of greater importance.

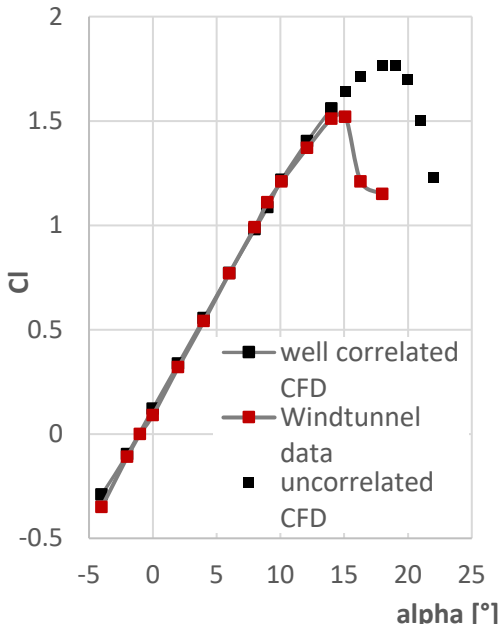


Figure 9 - Validation CFD framework (NACA data adapted from [21]).

Subsequently, the alpha polar was computed at a Reynolds Number of $2.6 \cdot 10^6$. As illustrated in Figure 9, the CFD simulations are able to precisely replicate the prevailing flow characteristics up to an angle of attack of 14°. However, the chosen CFD framework fails to predict stall accurately, which fits well to findings presented in literature [19]. Although the Spalart-Allmaras turbulence model would likely have matched the wind tunnel results more closely [19], it is not an option for the intended simulation due to its poor performance in predicting the effects of vortex generators [20]. Consequently, the following investigations had to be limited to the linear pre-stall region which is assumed to extend up to angle of 14 degrees. Since the subsequent analysis is performed at a higher Reynolds Number which causes the flow to remain attached up to slightly larger angles of attack this assumption should be conservative.

**Mesh topology 2D airfoil with extended flap:**
In order to capture the flow physic of a slotted flap additional mesh refinements were implemented. The circumferential area around the main wing trailing edges were refined as well as the entire flap bay. Furthermore, the flap wake was refined accounting for a possible separation of the flap. Moreover, the flap itself was refined in the same manner as the wing.

**Mesh toptology 2.5D airfoil section with installed VGs**
Performing a CFD optimisation asks for a high degree of automatisation. This is especially true for the mesh generation. To this end, a fully parametrised CAD model of the airfoil section and the vortex generators was created using the direct design parameters. Configuration control is facilitated by a design table, which was generated using the Latin Hypercube sampling plan and the design space boundaries defined. In addition, the CAD-model also includes all sizing and refinement regions which scale automatically depending on the respective VG design parameter combination. Furthermore, a predefined size field could be imported into ANSYS FLUENT Meshing which allocated predefined values to the respective refinement regions. This way the creation of flow domain and refinement region only required a single click in the CAD model and the mesh generation in ANSYS FLUENT Meshing utilizing sizing field and CAD model could be conducted by a small script.
All refinement regions of the 2D airfoil model with extended flap were also used for the 2.5D model. However, further refinements were added to capture the prevalent flow phenomena such as vortex shedding and propagation accurately. The highest grid resolution is needed at the VG edges which is

why cell size was limited here explicitly. Moreover, a box enclosing the vortex generators was defined to ensure high resolution in direct vicinity of the VGs. This refinement region then merges with the slightly coarser VG wake region (Figure 10). The height of the VG wake refinement was configured to be 6 h, in accordance with experimental findings in [5].

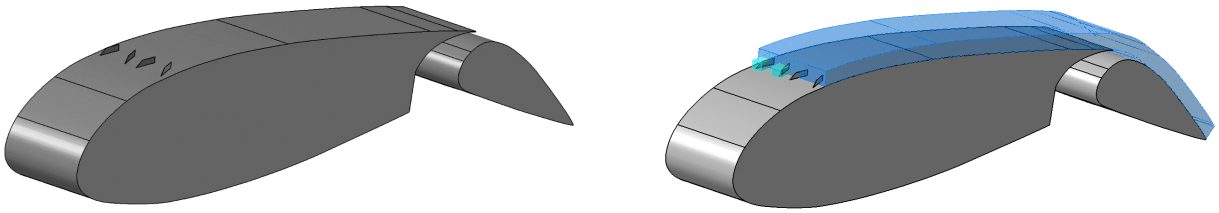

Figure 30 - 3D Inboard CAD model with installed VGs.

The prism layers on main wing and flap were defined exactly as for the 2D pre-calculations. However, prism layers also had to be placed on the VG surfaces. Since the vortex generators may be submerged in the boundary layer for some configurations, proportions between the total prism layer height and VG size are quite unfavourable. Consequently, a compromise had to be found between being able to mesh the vortex generators with acceptable cell quality and being able to at least resolve the laminar sublayer on the airfoil. In the vicinity of the vortex generators the thickness of the prism layer was thus reduced significantly (Figure 11). While this approach introduces the potential for poor quality cells at the interface between poly and prism cells where the prism layer thickness gradually reduces, it represents a suitable approach for automatic mesh generation of submerged vortex generators. The resulting gap in the prism layer where the vortex generators sit was meshed using polyhedral cells.

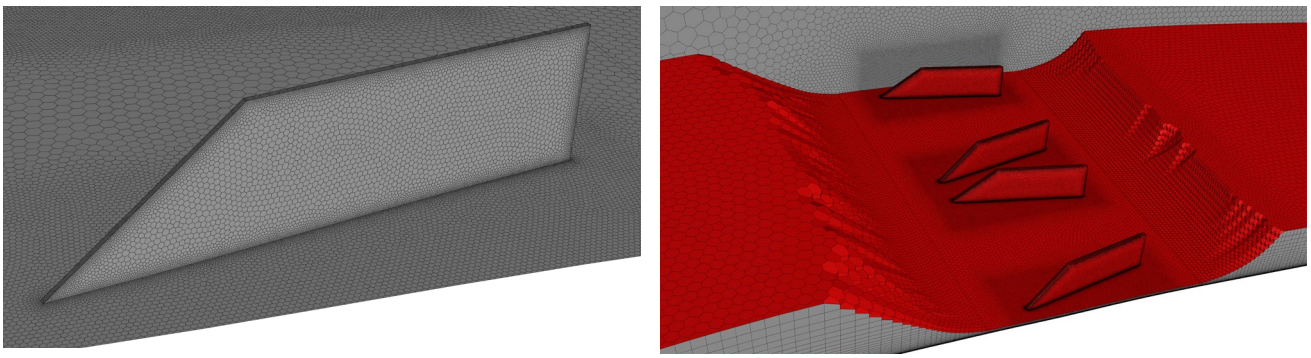

Figure 31 - Mesh refinement around VGs.

The general mesh topology was iterated to achieve an optimal result in terms of quality and cell count. Figure 12 shows the final mesh. The refinement of the main wake and the flap wake are clearly visible as well as the local VG refinements.

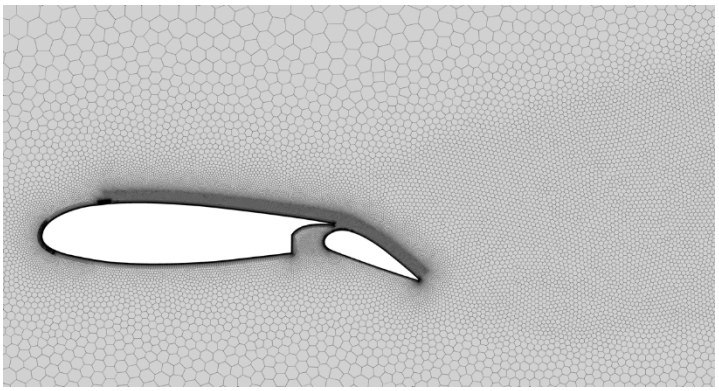

Figure 12 - Optimised polyhedral mesh showing the various refinement zones.

In an early version, four vortex generators, i.e. one full pair and two half pairs in conjunction with periodic boundary conditions, were placed on the wing to directly model the mutual vortex interference within the flow domain rather than relying on the periodic boundary conditions. However, investigations showed that the outer VGs (half pairs) could be omitted since the periodic boundary condition proved to capture the interference just as well as directly modelling the vortices. This allowed to almost half the required cells. For visual representation, the version with 4

vortex generators is used in this paper.
The final mesh size ranges from about 2 million cells up to 10 million cells. This variation is mainly caused by a change in span depending on the respective design parameter combination. A large VG height combined with a large spacing between VG pairs caused maximum cell counts.

## 5. Aerodynamic evaluation of the baseline wing

The cross-sectional shape of the wing with flap was determined using laser scanning on a real Cessna 208 aircraft. This was necessary to get the correct geometry particularly in the airfoil – flap gap area. An inboard section (WS 35) and an outboard section (WS 226) were scanned as shown in Figure 13.

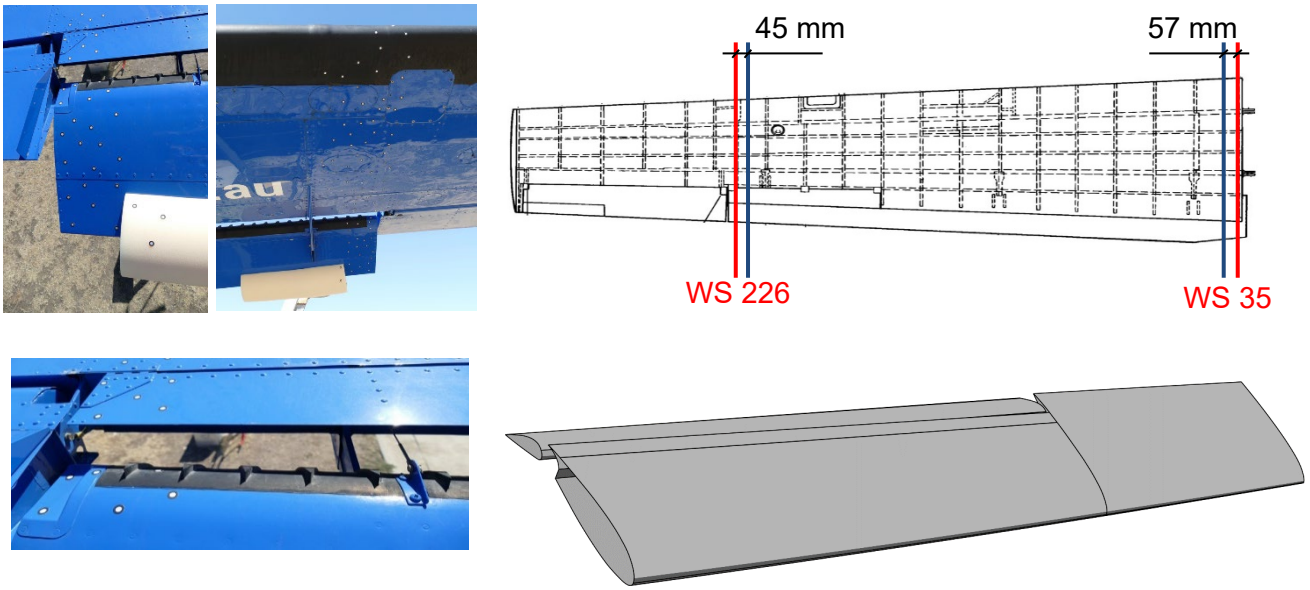


Figure 13 – Spanwise airfoil sections investigated.

In combination with data found in literature and manuals it was possible to reverse engineer the jig shape of the Cessna 208 wing.

### Aerodynamic Evaluation of the Outboard Airfoil (WS 226)

Investigations were performed at a Re = $3.1 \cdot 10^6$ based on the clean wing chord (1.453 m). The free stream velocity was set to 113 km/h (aircraft stall speed) and the flap was fully extended. The resulting polars are presented in Figure 14. As was established during the validation of the CFD framework, angles of attack greater than 14° were excluded from this study and are labelled accordingly in the aerodynamic polars.
The steady-state simulations deliver unreliable results due to a strong flow separation at the upper side of the flap (Figure 15). At certain angles of attack the separation even start to oscillate forming a Karman Vortex Street. In contrast, transient simulations can capture the prevailing flow

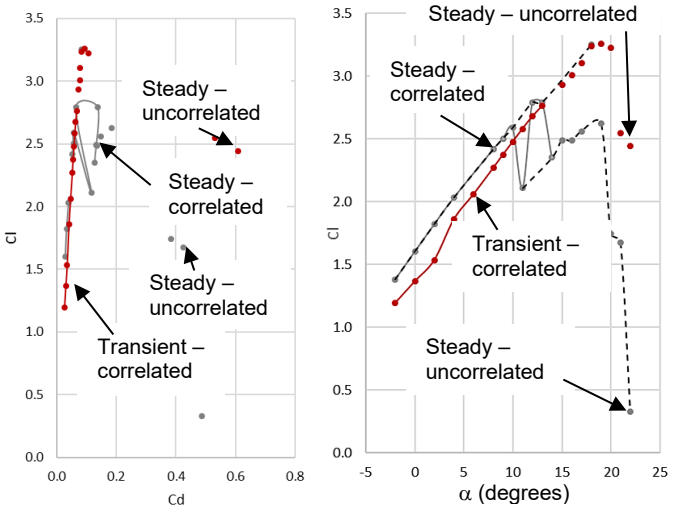


Figure 14 – Aerodynamic polars outboard section (WS 226).

conditions more accurately delivering reasonable polars. Interestingly the flow over the flap is still partially detached at higher angles of attack such as 11°. While high-lift systems show an affinity for flow separation on the flaps at low angles of attack flow separation at this angle of attack hints at sub-optimal inflow conditions due to either gap geometry or size [2]. Since the k-omega SST turbulence model tends to delay separation compared to experimental results [19], the flap is likely stalled as well. The fact Cessna offers a vortex generator kit exactly for the spanwise location investigated here makes it quite likely flow separation can also be observed in flight conditions.

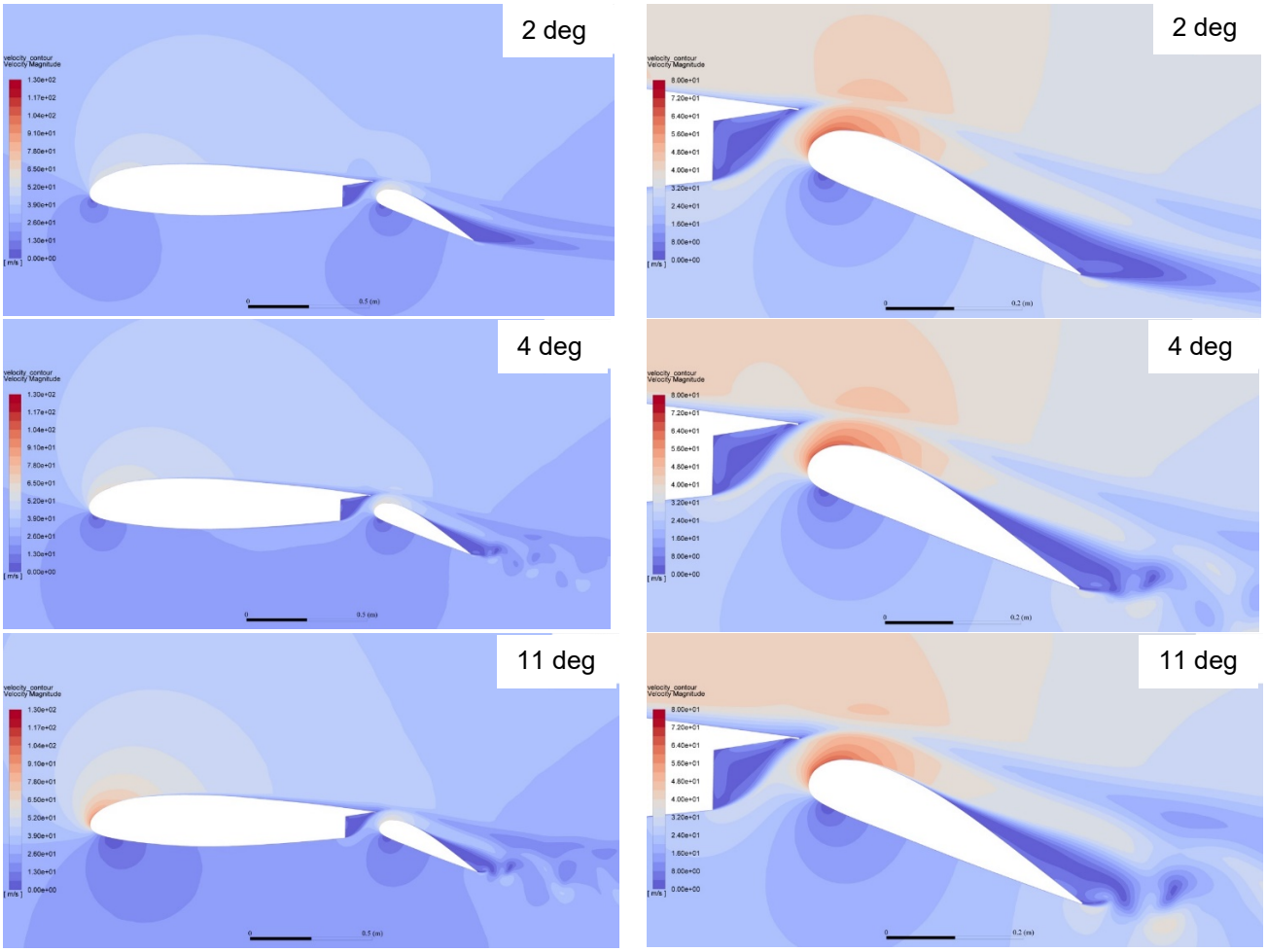


Figure 15 – Velocity contours for outboard airfoil with flaps extended and different angles of attack.

To analyse the optimisation potential, the development of the boundary layer velocity profile was examined for different angles of attack (Figure 16). Although a degradation of the velocity profile can be observed with increasing angle of attack, no flow reversal occurs even at larger angles of attack such as 11°. Consequently, it is unlikely to achieve any measurable stall speed reduction by placing VGs on the main wing of this outboard section.

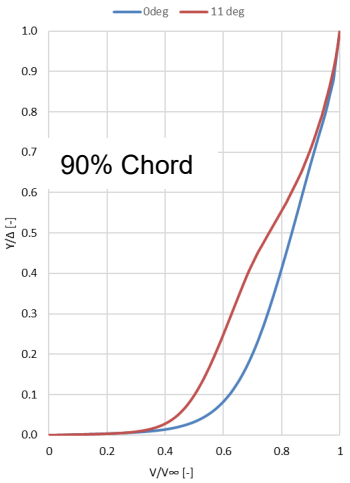


Figure 16 – Boundary Laver Profiles (WS 226).

**Aerodynamic Evaluation of the Inboard Airfoil (WS 35)**

Investigations were performed at a Re = $4.2 \cdot 10^6$ based on the clean wing chord (1.974 m). Again, the free stream velocity was set to 113 km/h and the flap was fully extended. The resulting polars are presented in Figure 18. In contrast to the outboard airfoil, no transient calculations were required for the inboard airfoil. The inboard section shows only very moderate flow separation on the flap, as shown in Figure 17. This can

be attributed to better inflow conditions, as the main wing is free from secondary control surfaces at this section, further underpinning the findings outlined in the previous subchapter regarding the flap-mounted vortex generator retrofits. Little to no flow separation occurs on the flap and the flow over the main wing remains attached up until 13°. The confluent boundary layer on the flap and the turbulent wake of the main wing are very prominent at 13°. These phenomena are corroborated by multiple numerical studies performed on high lift devices supporting the validity of the CFD framework [13][14].

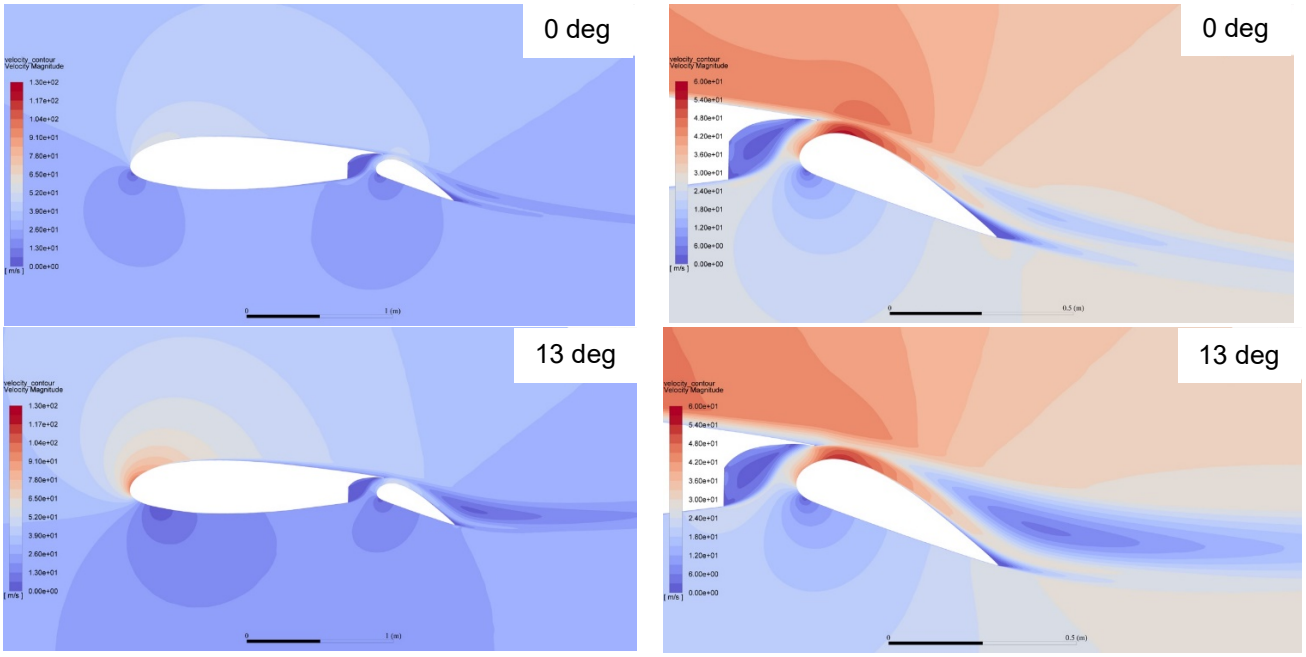


Figure 17 – Velocity contours for inboard airfoil with flaps extended and different angles of attack.

The velocity contour plots also show minimal optimisation potential for this airfoil section, particularly since flap flow remains attached across the angle of attack range. This is underpinned by the boundary layer velocity profiles which show no flow reversal hinting at flow separation onset (Figure 19).

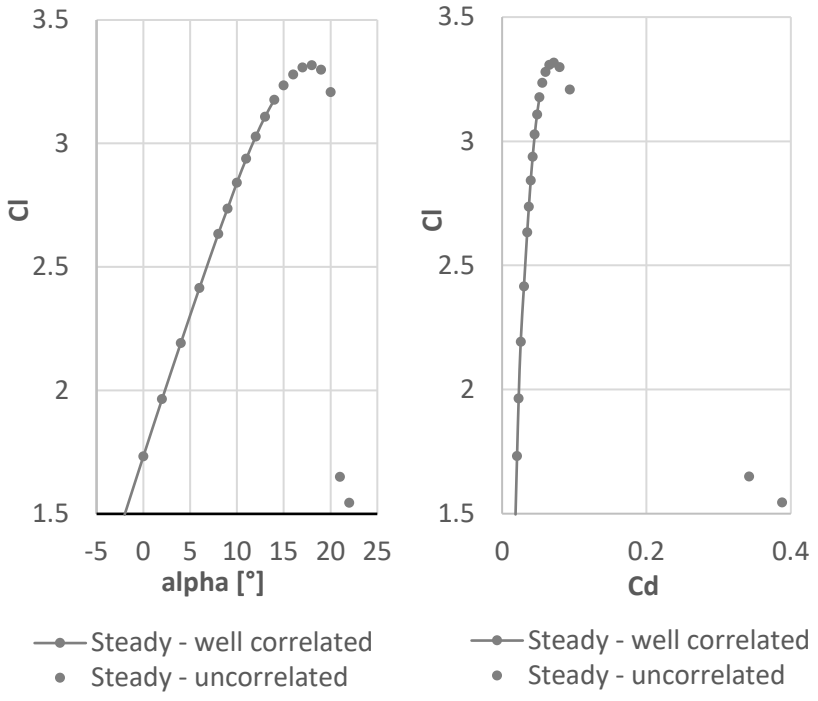


Figure 18 - Aerodynamic polars inboard airfoil WS 35.

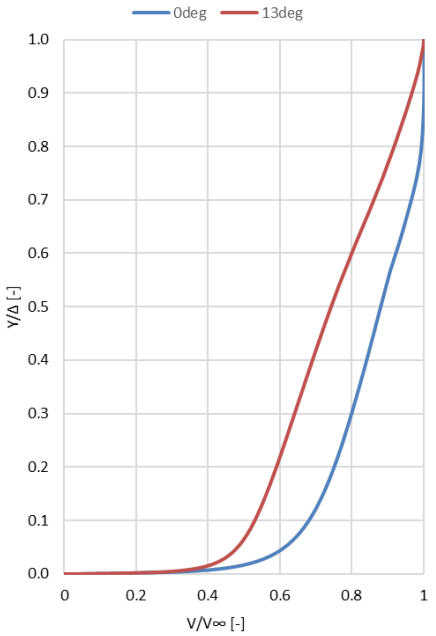


Figure 19 – Boundary layer profiles (WS 35) at 90 % chord.

## 6. Scope of optimisation

Performing numerical optimisation of a VG arrangement for an entire wing is an enticing idea. However, due to phenomena such as cross flow each VG pair would have to be optimised individually creating a design space in excess of 100 dimensions. Such an optimisation is not feasible in combination with high fidelity CFD simulations.

A reasonable simplification to cut down the enormous computational demands would be the separate optimisation of a VG design for a 2.5 D inboard and a 2.5 D outboard section. Here incorporation of crossflow conditions by appropriate pressure boundaries gained from clean finite wing simulations would be desirable. Subsequently, a linear interpolation between these two VG designs could deliver a VG design for the entire aircraft. However, the computational demands associated with this concept remain excessive. Trapezoidal counter-rotating vane type VGs were identified as most promising for the intended application. Other studies have pointed to a low influence of the design parameter length on performance and indicated a clear trend for the design parameter thickness. Choosing fixed values for these design parameters causes a minimum of five design parameters to remain for a complete optimisation of a VG pair, namely height, orientation, chordwise position, spacing within a pair and spacing between VG pairs. Based on what Gano, Kim and Brown [15] found in their Kriging study for a four-dimensional problem, a five dimensional problem would require an order of magnitude of no less than 500 simulations to build a model of suitable quality. If several objectives at different operational states are to be optimised, e.g. low drag at cruise and high lift at a large angle of attack, the number of required simulations is multiplied by the number of operational states to be considered. Performing this optimisation for 2 airfoil sections doubles the required number of simulations again. Consequently, optimising two airfoil sections for two operational states would require at least 2000 simulations. It must be emphasised that the stated numbers are only an educated guess. The number of required simulations is influenced significantly by the complexity of the multidimensional relationship – which obviously is unknown. However, although it is not possible to tell how many simulations are actually required, the number of simulations is likely beyond the scope of an optimisation study such as this considering the high cell size required to resolve the flow induced by vortex generators. Furthermore, it defies logic to perform such a high number of simulations without first investigating the potential of such an undertaking, which seems to be limited as shown by the baseline investigations.

This project is aiming for an exploration of the potential for lift increase at low speeds for the Cessna 208 by a retrofit of passive vortex generators. Consequently, the optimisation was limited to one airfoil section and the single objective to improve lift at the original stall speed and at a high angle of attack with fully extended flaps. However, this only reduces the number of required simulations by a factor of four, requiring further simplification. There are three options to further cut down the computational demands. First the mesh size could be reduced significantly which would entail losing the capability to accurately resolve the flow reenergisation by VGs. Secondly a reduced number of simulations could be conducted leading to a poor Kriging model quality. Thirdly the number of design parameters could be decreased to four. While the first two options would lead to results with little physical relevance the third option “only” involves the danger of missing the optimal solution and thus seems to be the only acceptable simplification to be made. Although all five design parameters are highly interdependent (refer to Figure 3) the design parameters height, orientation, spacing within a VG pair and spacing between VG pairs are more closely coupled. They determine the range of efficacy of the created vortices by controlling their size as well as the spacing between them. Thus, the subsequent optimisation will be performed for a fixed chordwise position with a VG installation at 20 % chord of the main wing as educated guess. This position combines low airfoil curvature, high kinetic energy input and minimal degradation of the stall behaviour. From the literature review individual optimisation ranges for the design parameters were determined that maximise the likelihood of including the optimal VG design in the design space. The corresponding optimisation boundaries are presented in Table 2.

Table 2 - Selected Optimisation Parameters and Range.

| | |
|---|---|
| Type (fixed) | spaced counter-rotating trapezoidal vanes |
| Length (fixed) | $4h$ |
| Thickness (fixed) | $0.5\ mm$ |
| Height | $0.5\ \delta - 1.8\ \delta$ |
| Orientation | 8° to +18° |
| Chordwise position (fixed) | 20% chord main wing |
| Spacing between VG pairs | $4.5h - 10h$ |
| Spacing within a VG pair | $1h - 2.5h$ |

Care had to be taken, that the design space boundaries are not mutually exclusive, e.g. the VG trailing edges of neighbouring VG pairs must be separated enough to allow for the prism layer to be generated around the VGs. Further, the inboard section was chosen for the optimisation. While the potential for aerodynamic improvement was deemed to be equally low as the outboard section, the scanned inboard section is representative of about 50 % of the wing due the arrangement of secondary control surfaces. In contrast, the outboard section is only representative of the spoiler region which has a modified flap bay geometry. Moreover, for the inboard section jib shape and flying shape should be almost identical, thus the inboard section allows for the investigation of the actual flying shape. Additionally, an angle of attack of 14 degrees was defined for the high lift optimisation as this is the largest angle that could be validated against wind tunnel data.

## 7. Vortex Generator Optimisation

To find an optimal VG design or trends for an optimal region, a Kriging model based on 60 sampling points was built and subsequently optimised. The individual steps of the optimisation process are described in the following sections.

In order to provide some further reassurance for the CFD-framework and modelling approach, a sample simulation of the vortex flow was compared to experimental data obtained by Ashill et al. [15].

CFD result

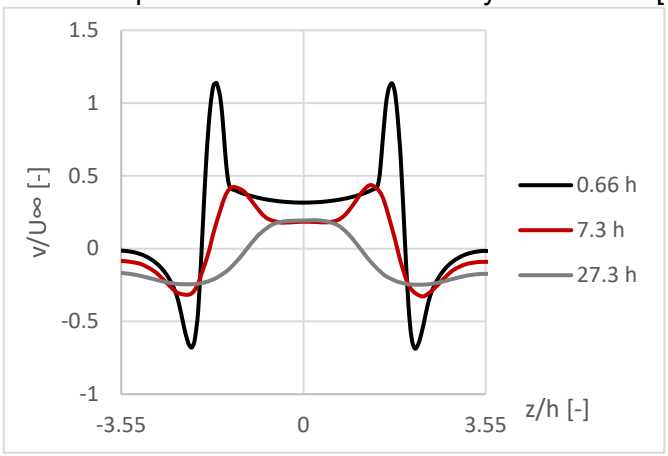


Wind tunnel result

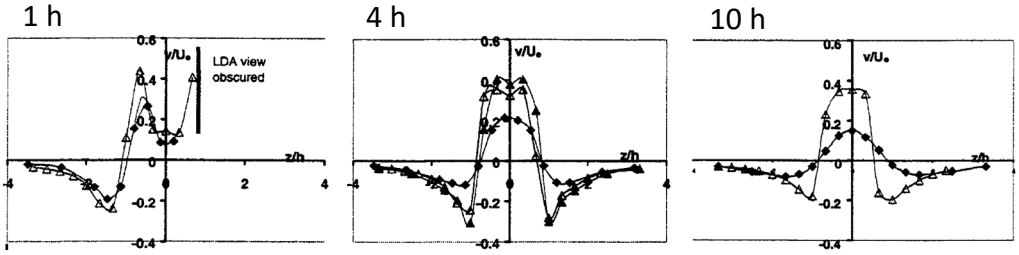


Figure 20 - Surface normal velocity induced by VGs for CFD and wind tunnel tests [5].

Figure 20 shows the surface normal velocity distribution (or up- and downwash velocity) at several streamwise locations downstream of the vortex generators for both numerical data obtained in this study

and experimental data. The similarities in velocity distributions hint at suitable accuracy with regard to the physical representation of the streamwise vortex development. Further, the vortex cores show similar lateral movement as denoted by the intersections with the horizontal axis. Relatively lower vortex decay of in the numerical model compared to the experimental data hints at decent vortex generator design, especially considering that the k-omega SST turbulence model tends to under predict streamwise vortex strength [20].

Apart from the numerical model, the quality of the Kriging model has a decisive influence on the validity of the optimisation result. The Kriging model was validated against a smaller subset of data. This data was obtained using the more computationally expensive CFD models with 2 VG pairs, which were replaced by a more efficient approach soon after. The validation revealed moderate agreement of the predictions (Figure 21), however, well within limits for the analysis of general trends. The average absolute error determined with the cross-validation data was a deviation of $\Delta C_L$ of 0.34%.

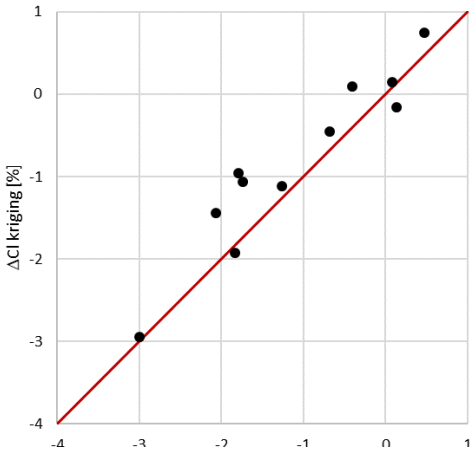


Figure 21 – Validation Kriging surrogate model.

The Kriging model was used in conjunction with a particle swam optimisation algorithm to predict global optima in the design space. The optimisation algorithm was tuned to be suitable for four dimensional problems by evaluating the Shekel function. A swarm size of 300 particles reliably delivered accurate results. Consequently, it was possible to prove the reliability of the numerical setup, compromising CFD, Kriging surrogate modelling and particle swarm optimisation.

Figure 23 visualises the four-dimensional Kriging model and thus shows the results of the entire optimisation. For each of the nine diagrams the design parameters height and orientation are fixed while the ordinate represents the optimisation range of the design parameter spacing within one VG pair and the abscissa accordingly for the spacing between VG pairs. However, the constant value assumed for height and orientation grows between the diagrams as indicated by the arrows. Finally applying the particle swarm optimisation on the Kriging model, a maximum lift increase of 1.22 % was found for the parameters compiled in Table 3 and Figure 22. This corroborates the assumptions about the low potential for lift increase outlined in the previous chapters.

Table 3 - Overview of optimal direct design parameters

| Design Parameter | Latin Hypercube Value | Design Space |
|---|---|---|
| Height | 1.13 | 9.4 mm |
| Orientation | 18 ° | 18 ° |
| Spacing within a VG pair | 2.5 h | 23.5 mm |
| Spacing between pairs | 7.62 h | 71.66 mm |

Interestingly only a very moderate improvement of lift was achieved, while the potential degradation was fourfold. The results for the VG spacing and the spacing of VG pairs is within range of previously conducted numerical and experimental studies, identifying an even spacing as extremely beneficial. An optimal VG spacing of about 2.5 h was also identified by other studies, such as [16] (numerical) and [17] (experimental). The optimal spacing of VG pairs of 6 h, near the optimum found in this study, was also found in other studies.

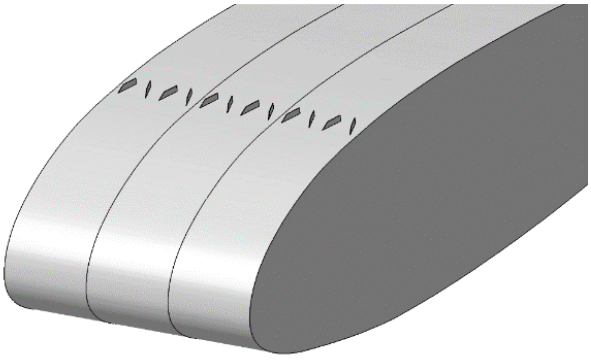

Figure 22 - Optimal vortex generator design.

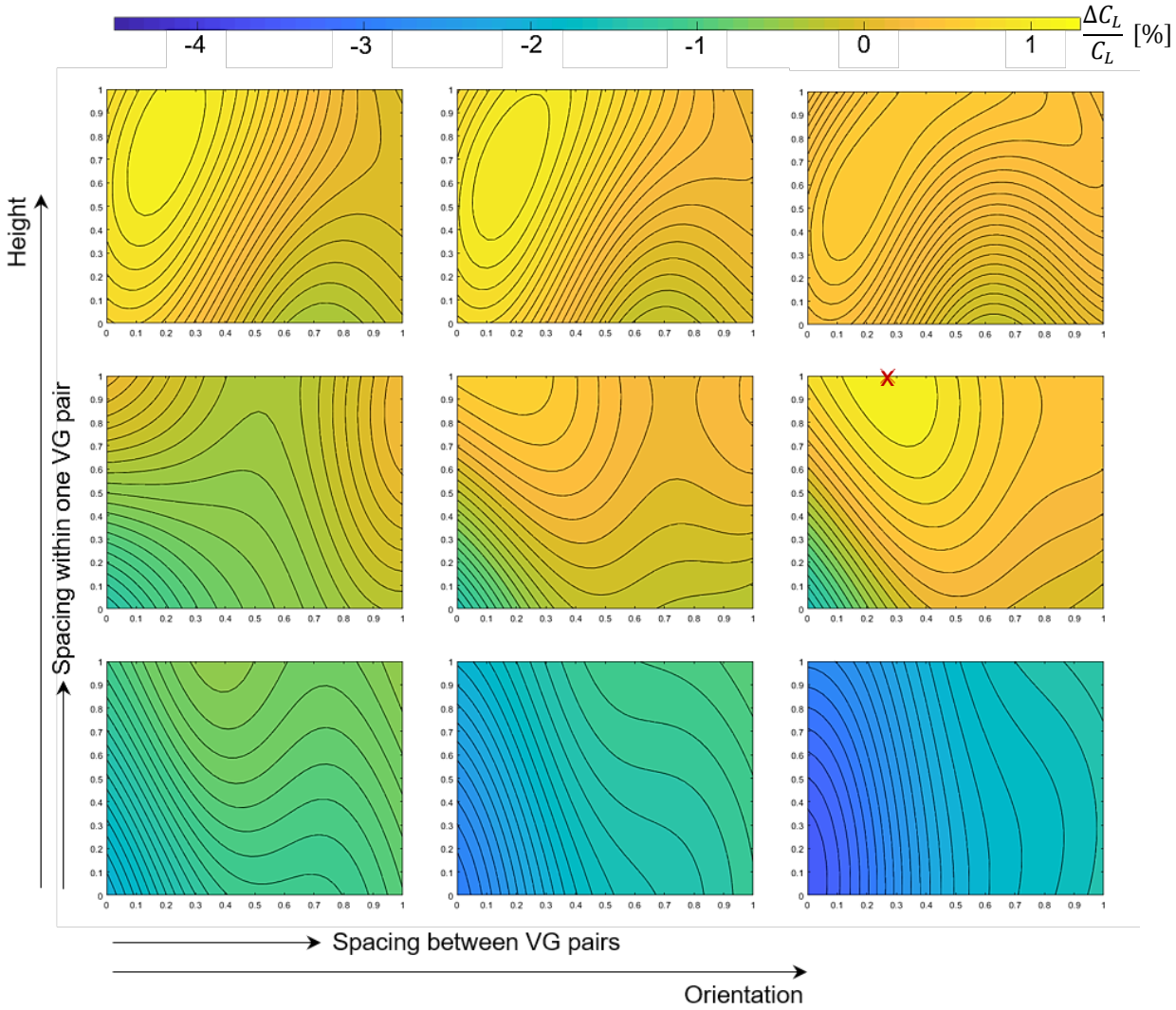


Figure 22 - VG spacing and the spacing between pairs with varying height and orientation.

The in-depth analysis of the connections between the four direct design parameters shows a strong dependency on the parameter height. Generally, with increasing height the efficacy of the vortex generators appears to be improved. At low to moderate VG heights, the adverse effect of a large incidence angles producing strong vortices coupled with low spacing between both VGs and VG pairs is particularly prominent. This can be attributed to the increased mutual interference between vortices. At lower heights interference with the wall-shear layer is increased as well.

Three local optima can be identified of which one is global. With increasing VG height, a lower VG inclination seems to be favourable which fits to the findings of Yao et al. [18]. This may be attributable to larger VGs stalling at lower angles of attack, thus reducing efficacy [18]. Quite clearly a VG spacing of 2.5 h is common for all optima, hinting at a general trend as corroborated by the studies outlined before.

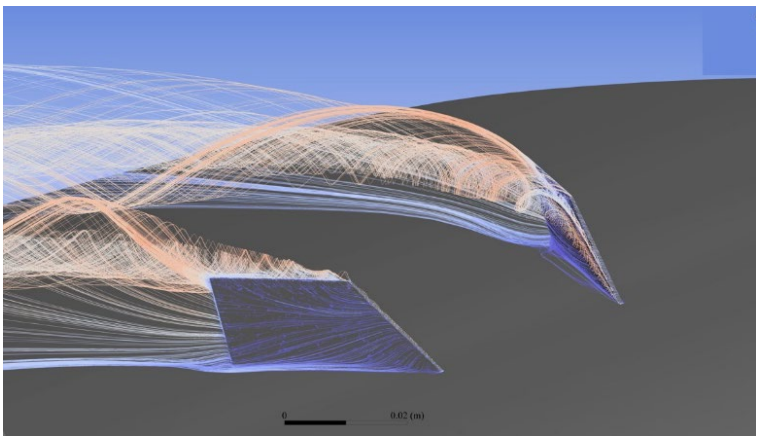

Figure 23 - Vortex Formation at the VG edges.

The analysis of the flow field behind the vortex generators (Figure 23) showed two separate vortex systems. A high energy vortex system originating from the leading edge of the vortex generator and a larger, lower energy system encapsulating the former. While this effect was not further investigated in this study it is assumed that while initial mixing may be increased, the excess interference within in this vortex system may be adversely affecting vortex strength decay. As all reviewed studies only compared different VG shapes (triangular, trapezoidal and rectangular) in terms of its impact on aerodynamic indices, an evaluation of the created vortex systems itself may offer further scope for research.

## 8. Conclusion

Eight geometric design parameters for the design of vortex generators were identified, which are: type, height, orientation, chordwise position, length, thickness, spacing within a VG pair and spacing between VG pairs. In order to guide vortex generator design in subsonic flow an allocation was presented how these geometric design parameters trigger three physical flow effects: range of efficacy, kinetic energy input and drag. Correct dimensioning of these design parameters is essential to avoid a degradation of the aerodynamic performance which shows the need for design optimisation. Furthermore, most of the design parameters are highly interdependent which makes a numerical optimisation the only reasonable approach.

In order to perform a sound optimisation based on valid results, accurate baseline geometry data is fundamental. 3D laser scanning was identified as a powerful approach to reverse-engineer the unknown jig shape of a wing. Subsequently, the current state of the Cessna 208 wing was analysed based on two representative cross-sections. The results suggest little potential for lift increase due to the installation of vortex generators on the main wing. However, it was found that the region of the flap behind the spoiler separates almost over the entire angle of attack range in contrast to the rest of the flap. Cessna offers a VG retrofit kit for exactly that part of the wing, increasing confidence in the numerical results. Consequently, installing this retrofit kit on the aircraft of MAF International is suggested to achieve a first lift increase. The deviation in aerodynamic performance between the different cross sections is caused by only a small modification of the slot geometry between the main wing and flap, highlighting the importance of the conducted 3D laser scanning to create meaningful results.

Subsequently, a VG optimisation for the scanned inboard section was performed at an angle of attack of 14° at stall speed in order to further investigate the optimisation potential of placing VGs on the main wing. However, in order to accommodate the high computational demands, set by accurate CFD simulations and the creation of a multidimensional Kriging surrogate model, the optimisation was limited to the design parameters height, orientation, spacing within a VG pair and spacing between VG pairs. While the literature review delivered evidence to confidently fix three design parameters, it would have been preferable to include the chordwise position in the optimisation procedure. The performed numerical optimisation confirmed the assumptions made in the aerodynamic baseline analysis. There is very limited potential for aerodynamic performance improvement of the Cessna 208 wing by installing vortex generators on the main wing. While most VG designs lead to a degradation of the aerodynamic performance, the optimal solution only suggested a lift improvement of 1.2%.

However, the performed optimisation gave interesting insights into the interaction of the optimised design parameters which may help to enhance the understanding of vortex generators. Optimisation pointed towards a design with equally spaced VGs. This way vortices are more separated reducing rapid vortex decay due to mutual interference and thus creating a long range of efficacy. As other studies yielded similar results a equal VG spacing might be a good design rule to follow as long as a large range of efficacy is desired. Furthermore, the findings suggest to reduce the VG incidence angle with increasing height.

## 9. References


[1] MAF International: https://www.maf.org/

[2] Lin, JC Review of Research on Low-Profile Vortex Generators to Control Boundary-Layer Separation, *Progress in Aerospace Sciences* 38 389–420, 2002.

[3] Fouatih, OM, Medale, M, Imine, O & Imine, B Design Optimization of the Aerodynamic Passive Flow Control on NACA 4415 Airfoil using Vortex Generators, *European Journal of Mechanics - B/Fluids*, vol. 56, pp. 82-96, 2016.

[4] Ashill, P, Fulker, J & Hackett, K Research at DERA on Sub-Boundary Layer Vortex Generators (SBVGs), *39th AIAA Aerospace Sciences Meeting and Exhibit*, Reno, 2001.

[5] Ashill, P, Fulker, J & Hackett, K Studies of Flows Induced by Sub-Boundary Layer Vortex Generators (SBVGs), *40th AIAA Aerospace Sciences Meeting & Exhibit*, Reno, 2002.

[6] Lin, J Control of Turbulent Boundary-Layer Separation using Micro-Vortex Generators, *30th AIAA Fluid Dynamics Conference*, Norfolk,1999.

[7] Rao, D & Kariya, T Boundary-Layer Submerged Vortex Generators for Separation Control - An Exploratory Study, *1st AIAA National Fluid Dynamics Conference*, Cincinnati, 1988.

[8] Gámiz, UF Fluid Dynamic Characterization of Vortex Generators and Two-Dimensional Turbulent Wakes, PhD thesis, *Universitat Politècnica de Catalunya*, Barcelona, 2013.

[9] Kerho, M, Hutcherson, S, Blackwelder, RF & Liebeck, RH Vortex Generators used to Control Laminar Separation Bubbles, *AIAA Journal of Aircraft*, vol. 30, no. 3, pp. 315-319, 1993.

[10] Thomson, K & Schulze, E Delivering Fuel and Emissions Savings for the 777, *AERO Magazine*, no. 35, 2009.

[11] Micro AeroDynamics Inc. 2018b, VG Kits for Cessna, Micro AeroDynamics Inc., <https://microaero.com/category/vg-kits/cessna-vg-kits/>.

[12] Micro AeroDynamics Inc. 2018a, CESSNA 207 Series MICRO Vortex Generator Kit, Micro AeroDynamics Inc., viewed 10.08.2018.

[13] Narsipur, S, Pomeroy, B & Selig, M CFD Analysis of Multi-Element Airfoils for Wind Turbines, *30th AIAA Applied Aerodynamics Conference*, New Orleans, 2013.

[14] Ying, SX, Spaid, FW, McGinley, CB & Rumsey, CL Investigation of Confluent Boundary Layers in High-Lift Flows, *AIAA Journal of Aircraft*, vol. 36, no. 3, pp. 550-562, 1999.

[15] Gano, S, Kim, H & Brown, D Comparison of Three Surrogate Modelling Techniques: Datascape, Kriging, and Second Order Regression,*11th AIAA/ISSMO Multidisciplinary Analysis and Optimization Conference*, Portsmouth, 2006.

[16] Fox, J, Bil, C & Carrese, R Particle Swarm Optimization with Surrogate Modelling of Passive Vortex Generators, *55th AIAA Aerospace Sciences Meeting*, Grapevine, 2017.

[17] Godard, G & Stanislas, M Control of a Decelerating Boundary Layer. Part 1: Optimization of Passive Vortex Generators, *Aerospace Science and Technology*, vol. 10, no. 3, pp. 181-191, 2006.

[18] Yao, C, Lin, J & Allen, B Flowfield Measurement of Device-Induced Embedded Streamwise Vortex on a Flat Plate, *1st AIAA Flow Control Conference*, St. Louis, 2002.

[19] Shelton, A, Abras, J, Jurenko, R & Smith, M Improving the CFD Predictions of Airfoils in Stall, *43rd AIAA Aerospace Sciences Meeting and Exhibit*, Reno, 2005.

[20] Florentie, L, Van Zuijlen, A & Bijl, H Towards a Multi-Fidelity Approach for CFD Simulations of Vortex Generator Arrays, *6th European Conference on Computational Fluid Dynamics*, Barcelona, 2014.

[21] Tetervin, N Tests in the NACA Two-Dimensional Low-Turbulence Tunnel of Airfoil Sections Designed to have Small Pitching Moments and High Lift-Drag Ratios, *National Advisory Committee for Aeronautics*, CB 3I13, 1943.


## Contact Author Email Address

cees.bil@rmit.edu.au

## Copyright Statement